COMPRESSION AND SYNCHRONIZATION OF AN ULTRA-SHORT ELECTRON BEAM USING A THZ UNDULATOR INTERACTION*

J.T. Moody, R.K. Li, P. Musumeci, C.M. Scoby, and H. To
Department of Physics and Astronomy, UCLA, Los Angeles California, 90095,USA

Abstract

Injection of electron beams into laser driven picosecond scale accelerating structures demand highly synchronized electron beams with bunch lengths approaching the femtosecond scale. One-dimensional numerical studies of undulator interactions of 3.5 MeV sub-picosecond electron beams and THz pulse trains produced by optical rectification have shown substantial compression and a reduction in time of arrival jitter with respect to the accelerator drive laser from the scale of hundreds of fs to that of tens of fs. In this paper a THz undulator based compression and synchronization scheme is investigated.

INTRODUCTION

Advanced accelerators such as laser wakefield accelerators (LWFA) [1] with plasma densities on the order of 10^{16} cm^{-3} have pushed acceleration buckets down to the picosecond timescale. These high gradient structures typically use self injection methods that have a wide phase acceptance, resulting in beams with large energy spread.

Photoinjectors can produce well understood high brightness beams but suffer from rf phase jitter on the scale of 500 fs. This jitter makes reliable injection into short timescale accelerating structures impossible. To make direct injection into high frequency structures possible, the photoinjector beam must be both synchronized to an optimal accelerating phase and occupy a small region near that optimal phase. This demands a longitudinal phase space control that reduces the time of arrival (TOA) jitter relative to the drive laser and compresses the beam before injection. A THz inverse free electron (IFEL) interaction can be used as such a control.

COMPRESSION AND SYNCHRONIZATION SCHEME

The proposed method to compress and synchronize the electron beam is shown in Fig. 1. It begins by splitting the drive laser into three parts. One part goes to the photocathode to produce the electron beam, one part goes to make a THz pulse train, and the remaining laser goes to drive the accelerating structure with a controllable delay. The electrons, having acquired jitter due to the rf acceleration process, and the still synchronized THz pulse train interact through the undulator resulting in imprinting the laser's temporal information back onto the electron bunch, reducing the jitter as well as compressing it. We examine each element of the scheme.

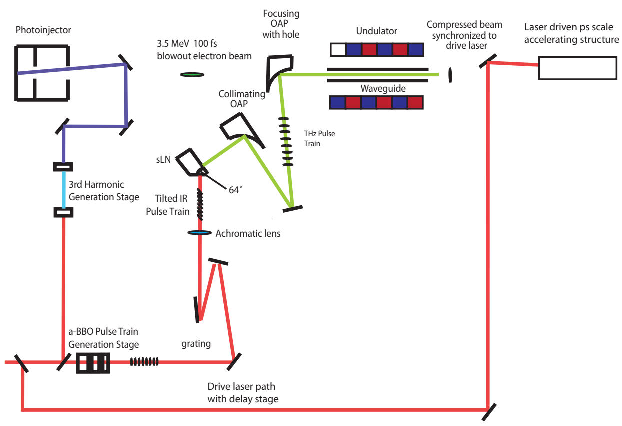

Figure 1: Diagram of the Compression and Synchronization Scheme

Initial Photoinjector Beam

The electron beam is modeled using the particle tracing code, General Particle Tracer (GPT) [2]. The beamline consists of a SLAC/UCLA/BNL 1.6 Cell S-Band photogun, a solenoid which acts as a lens, and a drift up to the undulator. To produce a sufficiently short beam, the photogun is operated in the blowout regime in which a 50 fs disk-like laser profile is applied to the photocathode, resulting in a space charge driven nonlinear longitudinal expansion into a near uniformly filled ellipsoidal distribution that is on the order of 100 fs rms [3]. This violent expansion occurs quickly, resulting in space charge forces that are linear, thus limiting emittance growth both transversely and longitudinally. The resulting beam is short, has a well defined chirp that is insensitive to charge fluctuations, and has a small slice energy spread, making the beam highly compressible [4]. The beam is focused to a 100 μm waist at the center of the undulator 1.07 m from the cathode. Further beam parameters are shown in Table 1.

THz Source

The THz pulse train is generated using the process of pulse front tilt optical rectification (OR) [5]. In OR, a broadband intense laser pulse impulsively drives a nonlinear crystal. Difference frequency mixing within the bandwidth of the laser pulse results in generation of low fre-

* This work supported by US ONR Grant N000140711174 and US DOE Grant DE-FG0292ER40693

quency radiation ranging from DC to several THz depending on the bandwidth of the laser pulse. At Pegasus, stoichiometric lithium niobate (sLN) is chosen as the nonlinear crystal due to its high effective nonlinear coefficient of 169 pm/V[6]. As with all nonlinear processes OR is strongly dependent on the phase matching condition, where the difference between the phase velocities of the laser and the generated THz radiation must be close to zero. Although the efficiency of OR scales as the square of the nonlinear coefficient, sLN suffers from a strong velocity mismatch between the 800 nm laser and the generated THz, which have respective indices of refraction of 2.25 and 4.96. To overcome the phase matching problem, the 800 nm drive laser pulse is tilted to the Cerenkov angle using a diffraction grating and imaged into the sLN crystal using an achromatic grating. The resulting THz is a near-single cycle pulse whose measured spectrum is shown in Fig. 2. At UCLA Pegasus laboratory, we have measured THz pulses with an energies of approximately 1 μJ from OR of 50 fs, 1 mJ 800 nm laser pulses with 30 nm of bandwidth.

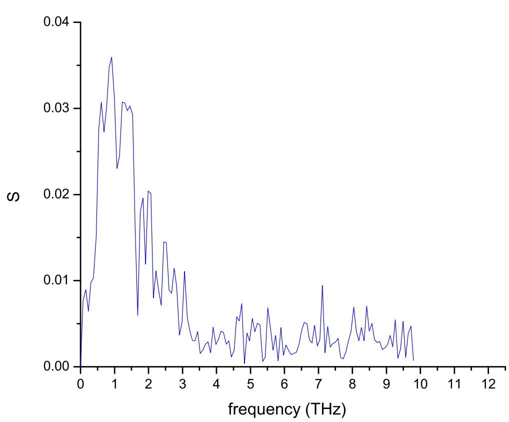

Figure 2: Spectrum of near single cycle THz pulse resulting from optical rectification

Single cycle pulses are insufficient to drive the undulator interaction as the electron beam stops interacting with the resonant spectral component of the THz radiation after one undulator period due to slippage between the laser pulse and the electrons. A THz pulse train overcomes the loss of interaction due to slippage by extending the radiation in time and can increase the spectral amplitude of the resonant THz by tuning the inter-pulse spacing. A THz pulse train can be produced by first running a 800 nm laser pulse through a series of birefringent crystals to create a laser pulse train with a desired spacing then sending it into the sLN crystal to undergo OR. The birefringent crystals split the laser pulse by propagating it in fast and slow modes, each with a different group velocity within the crystals. An 8 cycle pulse train containing approximately 2 μJ of energy in the resonant bandwidth is required to achieve sufficient coupling the electron beam to control the phase space. Experimental efforts are underway to further improve the efficiency of THz generation focusing particularly on the reduction of the high THz absorption in sLN by cooling it to liquid nitrogen temperatures.

Table 1: Compression Scheme Parameters

Beam Parameters	
Average γ	7
Normalized Emittance	.1 mm-mrad
Charge	1 pC
Undulator Parameters	
K	1.656
K_L	$4.21 \cdot 10^{-4}$
λ_w	1.77 cm
λ	430 μm
L_u	14.2 cm

THz Undulator Interaction

The undulator interaction is modeled by numerically integrating the IFEL 1-D equations of motions for the particles [7].

$$\frac{d\gamma}{dz} = \frac{1}{2\gamma} k K_L K JJ sin\Psi \tag{1}$$

$$\frac{d\Psi}{dz} = k_w - \frac{k}{2\gamma^2}(1 + \frac{K^2}{2}) \tag{2}$$

Here k is $2\pi/\lambda$, K_L is the radiation parameter equal to $eE_0\lambda/2\pi mc^2$ and E_0 is the peak radiation electric field, m is the electron mass, and c is the speed of light. K is the undulator strength parameter and is equal to $eB_w\lambda_w/2\pi mc^2$ and B_w is the peak undulator magnetic field. JJ is the coupling factor of the planar undulator γ is electron beam energy scaled by its rest mass, and Ψ is the pondermotive phase, defined by $(k + k_w)z - \omega t$. This model assumes a constant wavelength radiation source and, although we are using a pulse train to drive the compression and synchronization in the undulator which has a finite bandwidth, we note that only the resonant wavelengths of the THz radiation have an effect on the beam as the effects of non resonant modes will average to zero.

The undulator parameters values can be seen in Table 1. These parameters were selected to match the IFEL resonant condition, in which the pondermotive phase remains constant along the undulator:

$$k_w = \frac{k}{2\gamma^2}(1 + K^2/2) \tag{3}$$

γ is set by the average electron beam energy and k by the wavelength of THz produced through optical rectification. K and k_w are bounded by current magnet and machining technology with K selected near the upper bound as to maximize the pondermotive potential about the stationary phase, thus fixing k_w. With these parameters and a fixed

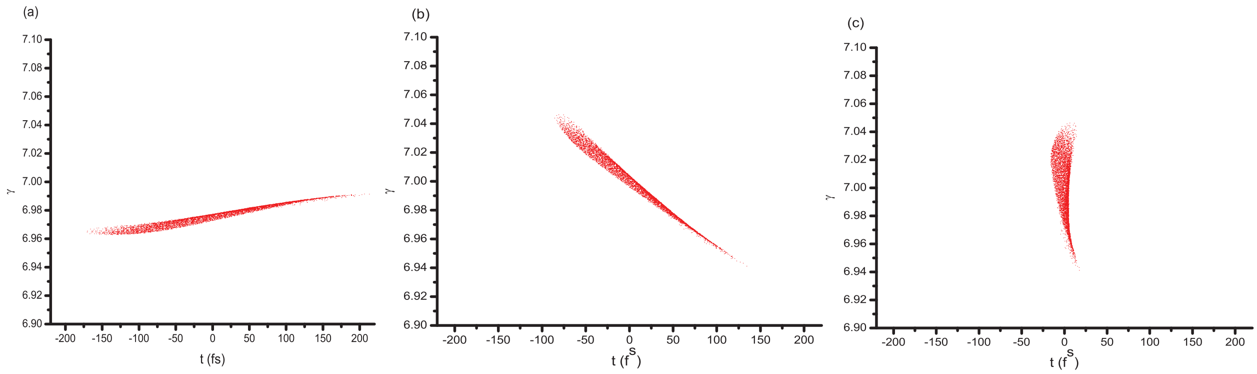

Figure 3: Longitudinal phase spaces of the beam at (a) the entrance of the undulator (b) the exit of the undulator (c) a 25 cm drift after the undulator exit

K_L assuming the above pulse train focused to a mm spot size, the equations of motion were numerically integrated using a fourth order Runge-Kutta method.

The compression effects can be seen in Fig. 3. The pondermotive potential near the stationary phase points cause a rotation in the phase space. Fig 3 (a) shows the initial longitudinal phase space (LPS) at the entrance of the undulator 1 meter from the cathode. Section (b) shows the resulting LPS at the exit of the undulator. The result of the interaction in the undulator is to place a negative linear chirp on the electron beam. Because the beam has relatively low energy, there is a significant positive R_{56} in the transport matrix for a drift section. After a 25 cm drift, the phase space rotates into a maximum compression, resulting optimally in a beam that is compressed a factor of 10.

To investigate synchronization, the final average pondermotive phase corresponding to a final time of arrival was examined as a function of the initial phase. The results of this study can be seen if Fig. 4 and show an order of magnitude reduction in time of arrival jitter, implying higher injection stability into a picosecond timescale accelerating structures.

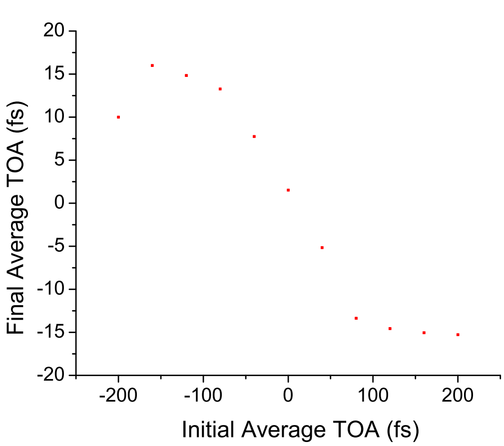

Figure 4: Time of arrival at undulator exit a function of time of arrival at undulator entrance.

CONCLUSION AND OUTLOOK

A one dimensional model for the THz undulator interaction has shown that neglecting transverse effects and space charge it is possible to create a beam suitable for injection into a laser driven picosecond timescale accelerating structure. This model assumed a fixed electric field strength along the undulator, which is inaccurate as the Rayleigh range is approximately 1 cm, an order of magnitude below the length of the undulator and the interaction is in the diffraction dominated regime. A solution to this is coupling the THz into a mm-scale waveguide[8]. At this size, the waveguide will be multimode, but the effect on the beam of other than resonant modes will likely average to zero. Current simulation efforts are directed at optimizing the interaction in a waveguide.

REFERENCES

[1] E. Esarey and C. Schroeder, Physics of Laser-Driven Plasma Acceleration, LBNL Report LBNL-53510 (2003)

[2] S.B. van der Geer, O.J. Luiten, M.J. de Loos, G. Pplau, U. van Rienen, 3D space-charge model for GPT simulations of high brightness electron bunches, Institute of Physics Conference Series, No. 175, (2005), p. 101.

[3] P. Musumeci et al., Experimental Generation and Characterization of Uniformly Filled Ellipsoidal Electron-Beam Distributions, PRL, 100/244801(2008).

[4] J. T. Moody et al., Phys. Rev. ST Accel. Beams 12, 070704 (2009).

[5] K.-L. Yeh, Generation of 10 μJ ultrashort terahertz pulses by optical rectification, Appl. Phys. Letters 90, 171121 (2007).

[6] J. Hebling et al., Generation of high-power terahertz pulses by tilted-pulse-front excitation and their application possibilites. J. Opt Soc Am B/Vol.25 No.7 (2008)

[7] E. D. Courant, C. Pellegrini, and W. Zakowicz. High-energy inverse free electron laser accelerator. Physical Review A, 32:2813, 1985.

[8] S.Reiche et al, Proposal for a IR waveguide SASE FEL at the Pegasus Injector, PAC Proceedings, 2001